

Late sodium current contributes to diastolic cell Ca^{2+} accumulation in chronic heart failure

Nidas A. Undrovinas · Victor A. Maltsev ·
Luiz Belardinelli · Hani N. Sabbah ·
Albertas Undrovinas

Received: 18 September 2009 / Accepted: 6 April 2010 / Published online: 19 May 2010
© The Physiological Society of Japan and Springer 2010

Abstract We elucidate the role of late Na^+ current (I_{NaL}) for diastolic intracellular Ca^{2+} (DCa) accumulation in chronic heart failure (HF). HF was induced in 19 dogs by multiple coronary artery microembolizations; 6 normal dogs served as control. Ca^{2+} transients were recorded in field-paced (0.25 or 1.5 Hz) fluo-4-loaded ventricular myocytes (VM). I_{NaL} and action potentials were recorded by patch-clamp. Failing VM, but not normal VM, exhibited (1) prolonged action potentials and Ca^{2+} transients at 0.25 Hz, (2) substantial DCa accumulation at 1.5 Hz, and (3) spontaneous Ca^{2+} releases, which occurred after 1.5 Hz stimulation trains in $\sim 31\%$ cases. Selective I_{NaL} blocker ranolazine (10 μM) or the prototypical Na^+ channel blocker tetrodotoxin (2 μM) reversibly improved function of failing VM. The DCa accumulation and the beneficial effect of I_{NaL} blockade were reproduced in silico using an

excitation-contraction coupling model. We conclude that I_{NaL} contributes to diastolic Ca^{2+} accumulation and spontaneous Ca^{2+} release in HF.

Keywords Action potential remodeling · Ca^{2+} handling · Heart failure · Na^+ current · $\text{Na}^+/\text{Ca}^{2+}$ exchange

Introduction

Congestive heart failure (HF) is associated with severe abnormalities in both cardiac rhythm and contractile function. While Ca^{2+} directly triggers contractions in cardiac myocytes, both cell Ca^{2+} content and dynamics are modulated by Na^+ ions [1]. Abnormal Na^+ handling and $\text{Na}^+/\text{Ca}^{2+}$ interplay in HF are being extensively investigated in order to develop new approaches to the treatment of HF [2–4]. While the majority of Na^+ channels open and inactivate during the action potential (AP) upstroke, some of them reopen during the AP plateau, carrying the so-called late or persistent Na^+ current (I_{NaL}) [5]. We found I_{NaL} in cardiomyocytes of both normal and failing human hearts [6], and further studies showed that I_{NaL} increases in HF, both in patients and in animal models [5, 7–9]. Augmented I_{NaL} plays an important role in impaired repolarization of cardiomyocytes of failing hearts [6, 7, 9–13].

Previous studies have suggested that during each beat a relatively small, but long lasting, I_{NaL} brings a substantial amount of Na^+ into cardiomyocytes, comparable to that carried by a large but very brief transient Na^+ current (I_{NaT}) [9]. The latter is reduced in chronic HF [8, 14, 15], whereas I_{NaL} is increased; hence, the relative contribution of I_{NaL} to the regulation of intracellular Na^+ is expected to increase further in myocytes from failing hearts. Thus I_{NaL} , by altering AP and providing Na^+ influx, might be

N. A. Undrovinas and V. A. Maltsev contributed equally to this work.

Electronic supplementary material The online version of this article (doi:10.1007/s12576-010-0092-0) contains supplementary material, which is available to authorized users.

N. A. Undrovinas · H. N. Sabbah · A. Undrovinas
Department of Internal Medicine, Henry Ford Hospital,
Detroit, MI, USA

V. A. Maltsev
National Institute on Aging, Intramural Research Program,
NIH, Baltimore, MD, USA

L. Belardinelli
Gilead Palo Alto, Inc., Palo Alto, CA, USA

A. Undrovinas (✉)
Cardiovascular Research, Henry Ford Hospital, Education and
Research Bldg. Room 4015, 2799 West Grand Boulevard,
Detroit, MI 48202-2689, USA
e-mail: aundrov1@hfhs.org

implicated in Na^+ -related Ca^{2+} overload, especially in the context of up-regulated $\text{Na}^+/\text{Ca}^{2+}$ exchanger (NCX) in HF [16–18]; reduced sarcoplasmic reticulum (SR), Ca^{2+} ATPase (SERCA), or Ca^{2+} -pump function; down-regulated Ca^{2+} -release channel (ryanodine receptor, RyR); and increased SR Ca^{2+} leak [18–23]. The increased I_{NaL} by depolarizing the cell membrane and increasing late Na^+ influx during AP is likely to facilitate a shift of the NCX operation in HF from the prime forward mode to the reverse mode, i.e., from Ca^{2+} efflux to Ca^{2+} entry [24], thereby contributing to cell Ca^{2+} accumulation in HF. Abnormal cell Ca^{2+} accumulation, in turn, worsens both contractility (via diastolic function) and rhythm (via spontaneous Ca^{2+} releases-triggered delayed after-depolarizations, DADs) [18, 25]. Therefore, inhibition of I_{NaL} could be a potential target to improve function of the failing heart, but this possibility remains largely unexplored. While some prior studies have indeed shown improved diastolic performance due to inhibition of I_{NaL} in different experimental conditions (including in vivo settings), those studies were mainly performed in a normal myocardium using pharmacological I_{NaL} enhancement with toxins or other Na^+ channel agonists [26–28], as well as expressing LQT-3 syndrome-related mutant Na^+ channels with retarded inactivation [29]. The properties of I_{NaL} in HF myocytes are distinctively different [9, 11, 12] from the non-inactivating I_{Na} produced by Na^+ channel agonists and mutations in myocytes of normal hearts (NH), not to mention differences in Ca^{2+} handling. Thus, the role of an augmented I_{NaL} in HF remains to be established.

Using a combination of experimental and numerical modeling approaches, the present study tested the hypothesis that I_{NaL} is indeed a major contributor to the dynamic, Na^+ -dependent diastolic Ca^{2+} (DCa) accumulation in single ventricular myocytes isolated from failing hearts. We used a canine chronic HF model that causes numerous physiological deficiencies similar to those observed in patients with HF [30]. Isolated single ventricular myocytes from failing hearts exhibited abnormal Ca^{2+} handling, including substantial DCa accumulation at a moderate-high physiological pacing rate of 1.5 Hz, which is deleterious to left ventricular ejection fraction in HF patients [31, 32]. Inhibition of I_{NaL} greatly reduced DCa and substantially decreased the probability of spontaneous Ca^{2+} releases (SCaRs), a well-known initiation mechanism of DADs and triggered arrhythmia [18, 25]. Our numerical modeling confirmed that I_{NaL} provides a substantial contribution to diastolic cell Ca^{2+} accumulation observed experimentally. Thus, inhibition of I_{NaL} may suppress a significant portion of the Ca^{2+} accumulation and decrease occurrence of SCaRs in cardiomyocytes and, thereby, is likely to improve heart contractility and rhythm in HF.

Methods

This study conforms to the guide of the care and use of laboratory animals published by the NIH and was approved by the Institutional Animal Care and Use Committee of the Henry Ford Health System. Our experimental methods, data analysis, theoretical formulations, and calculations are given in the Electronic Supplementary Material (ESM). In brief, chronic HF in dogs was induced by multiple sequential coronary microembolizations. Ca^{2+} signals were measured in field-stimulated, fluo-4-loaded single ventricular myocytes using a photo-multiplier; electrophysiological recordings were performed using the patch-clamp technique. Ca^{2+} signals and APs were measured at 35°C and 1.8 mM $[\text{Ca}^{2+}]_o$, I_{NaL} was measured at room temperature (21–23°C).

We used ranolazine (RAN) and tetrodotoxin (TTX) as pharmacological tools. Whereas TTX blocks both I_{NaT} and I_{NaL} equally [9], RAN blocks I_{NaL} preferentially [13]. RAN is superior to other Class I or III drugs (RAN > amiodarone > flecainide > mexiletine > lidocaine) [13, 33–36] at blocking I_{NaL} over I_{NaT} . Furthermore, RAN at the concentration of 10 μM used in the present study (i.e., close to therapeutic range of 2–8 μM) has only minor effects on K^+ currents [33], unlike amiodarone, which has major effects on K^+ currents. Concentrations of RAN (10 μM) and TTX (2 μM) were chosen to produce a comparable I_{NaL} inhibition (~ 1.5 of IC_{50}) based on our previous studies [9, 13].

Results are expressed as mean \pm SEM (if not stated otherwise), and statistical significance was based on $P < 0.05$, ANOVA followed by Bonferroni's post-hoc test. To evaluate the probability of the SCaRs we used non-parametric two-tailed Fisher's exact test.

We simulated the effect of selective inhibition of I_{NaL} on DCa accumulation and APs in silico using a modified excitation-contraction (E-C) coupling model of failing canine ventricular myocytes developed previously by Winslow et al. [37] (see details in the ESM).

Results

Minor effects of ranolazine and TTX on intracellular Ca^{2+} in myocytes from normal heart

First we tested the effects of 10 μM RAN and 2 μM TTX in field-stimulated cardiomyocytes of normal dogs on the duration (90%) of Ca^{2+} transients (CaT_{90}) and accumulation of DCa during a pulse train (see the ESM for definition) (Fig. 1). Both RAN and TTX only slightly reduced CaT_{90} at a low stimulation rate of 0.25 Hz, and these effects were not statistically different (Fig. 1c). At a high stimulation rate of 1.5 Hz, accumulation of DCa was negligible (a few percent) both in control and under RAN or TTX (Fig. 1b).

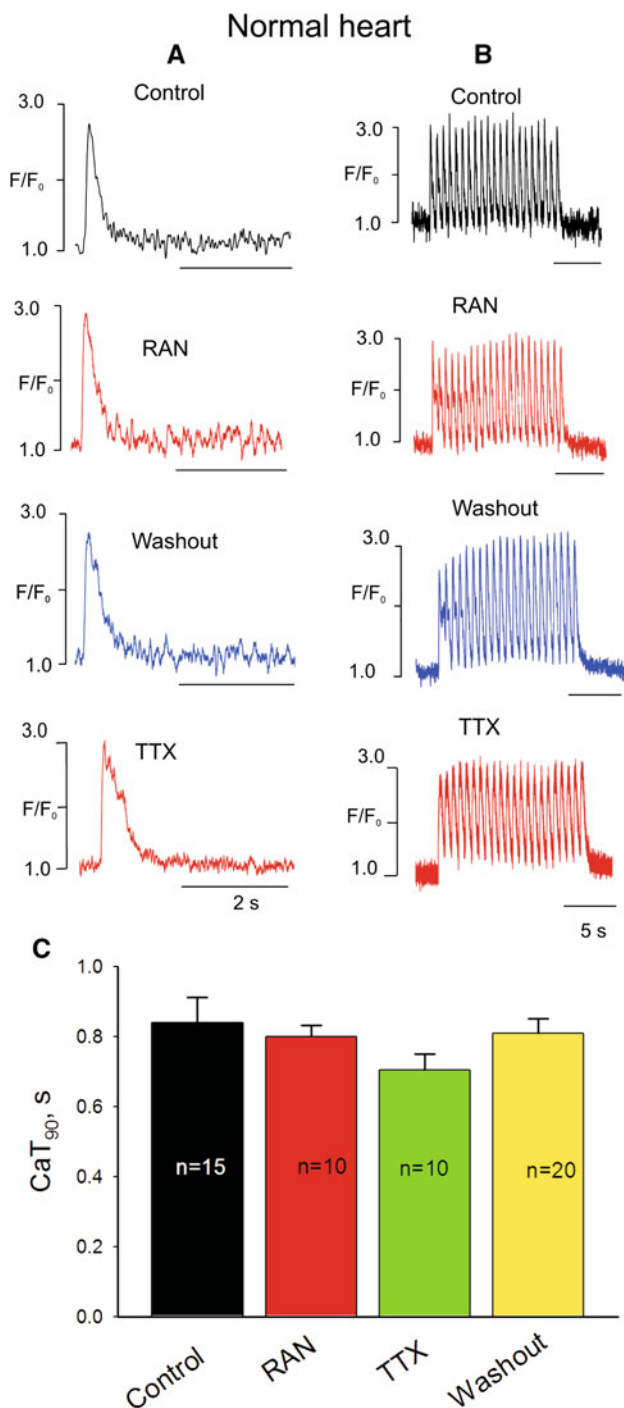


Fig. 1 Representative examples of Ca²⁺ transient recordings in normal dog heart ventricular myocytes at low (a) and high (b) pacing rates before and after infusion of ranolazine (RAN) or tetrodotoxin (TTX). c Data summary (mean ± SEM, n = 10–20) for Ca²⁺ transient duration (CaT₉₀)

Improvement of intracellular Ca²⁺ handling in myocytes from failing heart by TTX and ranolazine

Ca²⁺ transients were substantially different in field-stimulated myocytes of failing compared to normal heart.

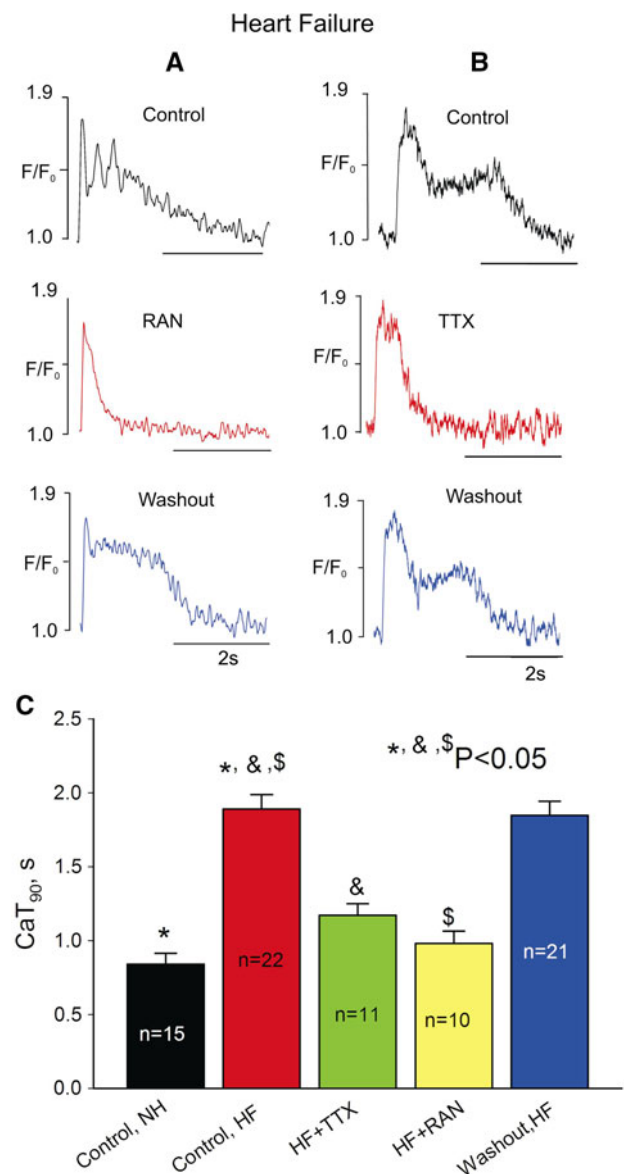


Fig. 2 Ranolazine and TTX shorten Ca²⁺ transient duration (CaT₉₀) in failing dog ventricular myocytes at low pacing rates (0.25 Hz). a, b Representative examples of Ca²⁺ transient recordings, c summary of the data (mean ± SEM, n = 10–22) for CaT₉₀

CaT₉₀ of failing myocytes was significantly longer, and the CaT had a spike-dome configuration when myocytes were stimulated at a frequency of 0.25 Hz (Fig. 2). Some failing myocytes exhibited multiple oscillations on top of the “dome” (Fig. 2a, upper panel). Both RAN and TTX improved CaT, as they significantly and reversibly shortened CaT₉₀ by suppressing the dome phase (Fig. 2c).

Increasing the stimulation rate to 1.5 Hz markedly increased the DCa level during the pulse train (Fig. 3a, b, upper panels) and induced beat-to-beat CaT alternations in amplitude and duration in all HF myocytes studied (Fig. 3a, upper panel). Both RAN (Fig. 3a) and TTX

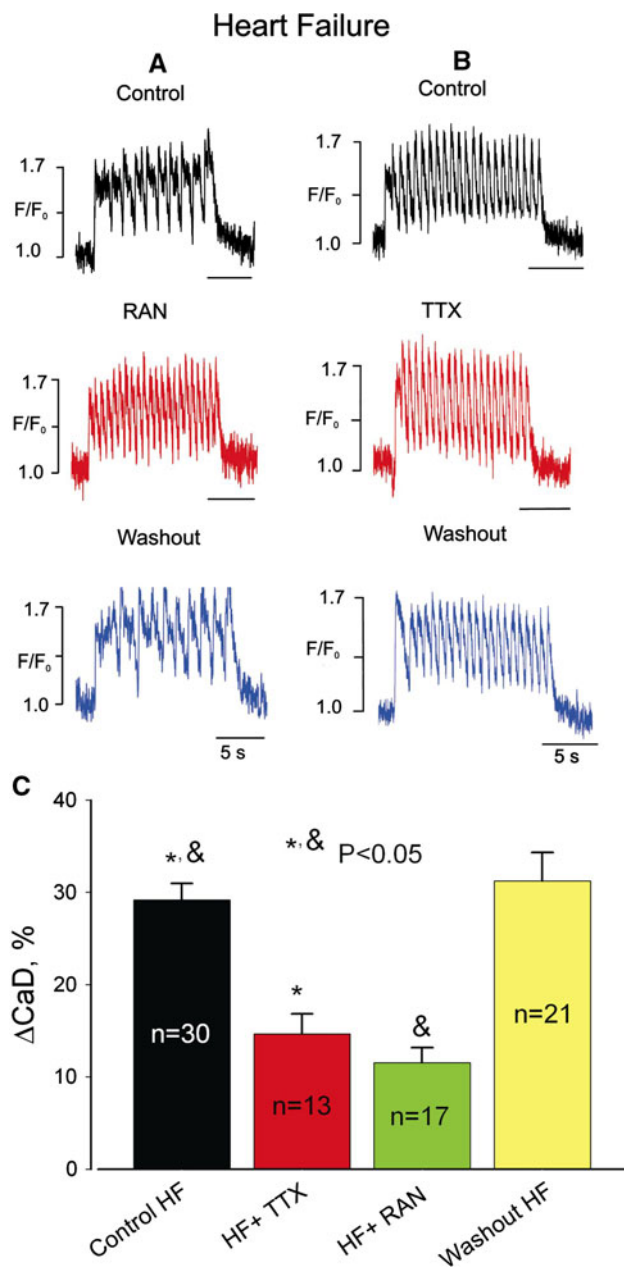


Fig. 3 Ranolazine and TTX reduce diastolic Ca²⁺ elevation at high pacing rates (1.5 Hz) in failing dog ventricular myocytes. **a**, **b** Representative examples of Ca²⁺ transient recordings, **c** data summary for diastolic Ca²⁺ (CaD) changes (ΔCaD) during a pulse train. Data are mean ± SEM pooled from 13 to 30 cells

(Fig. 3b) significantly and reversibly decreased DCa accumulation and eliminated these changes (Fig. 3c).

Next we determined whether failing myocytes generate SCaRs when subjected to 1.5 Hz trains of stimulation pulses. SCaRs occurred in ~31% of instances with a delay of 2.1 ± 0.2 s ($n = 17$) after the end of the last pulse of the 1.5 Hz train of pulses (Fig. 4a). SCaRs were absent in

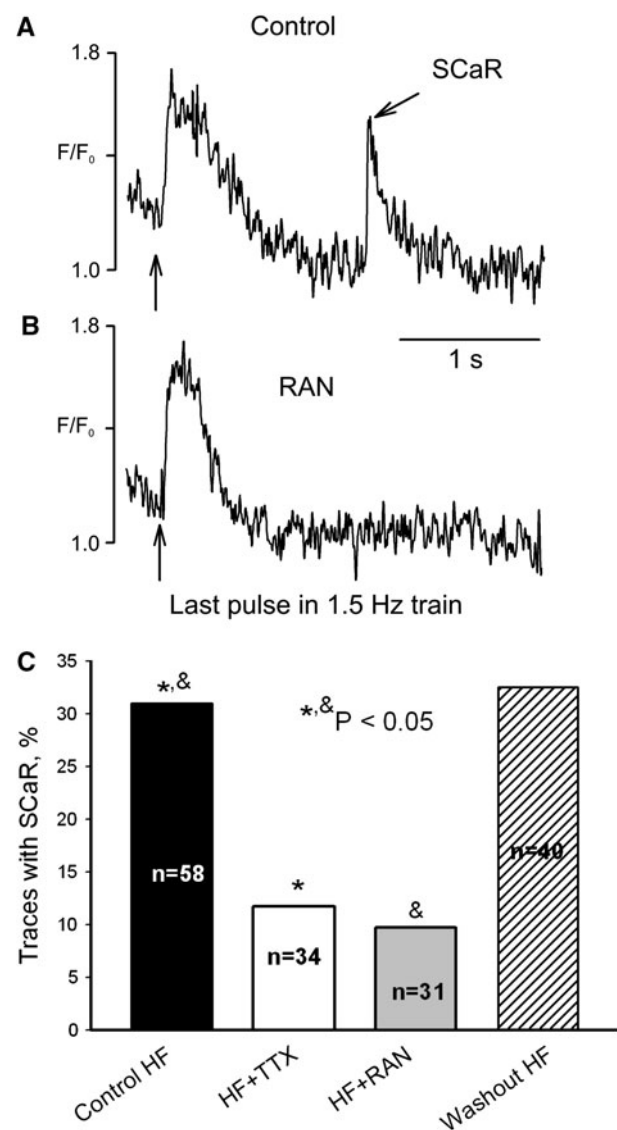


Fig. 4 Ranolazine prevents spontaneous Ca²⁺ releases (SCaR) in myocytes from failing dog heart. Representative traces of Ca²⁺ signals just after the 1.5 Hz pulse train **a** in control and **b** in the presence of 10 μM ranolazine (RAN). Vertical arrows indicate the last pulse in the train. **c** RAN significantly and reversibly decreases the rate of SCaR. The probability of SCaR occurrence (bars) was evaluated as the percentage of traces that contained SCaR (similar to that shown in **a**). In control conditions 18 out of total 58 traces contained SCaR, in TTX it was present in 4 out of total 34 traces, in RAN it was present in 3 out of 31 traces, and after washout it was present in 13 out of total 40 traces. Statistical comparison was performed using two-tailed Fisher's exact tests, and $P < 0.05$ was considered to be significant. Data were pooled from 31 to 58 cells

myocytes of NH. The SCaR amplitude was comparable to that of CaT within the pulse train (see below) and ranged from 163 to 251 nM (calculation of $[Ca^{2+}]_i$ is given in the ESM). Both TTX and RAN greatly (~threefold) and reversibly reduced the probability of SCaR occurrence (Fig. 4).

Does ranolazine affect SR Ca^{2+} content and NCX function?

The mechanism for the S Ca R s , which are precursors for DADs, is the interplay between the SR Ca^{2+} load, cytoplasmic $[\text{Ca}^{2+}]$, and NCX (see for review [25]). Therefore, in order to further address the mechanism of the beneficial effects of RAN to decrease the probability of S Ca R occurrence (Fig. 4), in the next experiments we determined SR Ca^{2+} content (or load) and NCX function by the caffeine-induced Ca^{2+} -transients at a basal stimulation rate of 1.5 Hz in the presence and absence of the drug. The amplitude of the caffeine-induced Ca^{2+} transient was used as a measure for SR Ca^{2+} load [28], and the decay time constant was used as an estimate of NCX activity [38]. Figure 5a shows traces of the caffeine-induced Ca^{2+} transients in the absence (left panel) and presence of RAN (10 μM , right panel). Figure 5b and c shows summary data of the caffeine-induced transient amplitude (SR Ca^{2+} content) and decay time constant (NCX function). Our data show that the decay kinetics (Fig. 5c) after RAN application changes insignificantly. Although there was an apparent reduction in SR Ca^{2+} load (Fig. 5b), the statistical analysis does not reveal statistically significant difference in caffeine-induced Ca^{2+} transient amplitude (Fig. 5b). Therefore, we assumed that RAN affects neither SR Ca^{2+} load nor NCX function.

Effects of ranolazine on I_{NaL} in myocytes from failing heart

In our previous study we have shown that RAN preferentially blocked I_{NaL} ($\text{IC}_{50} = 6.46 \mu\text{M}$, for HF) over I_{NaT} ($\text{IC}_{50} = 294 \mu\text{M}$, NH; $\text{IC}_{50} = 244 \mu\text{M}$, HF) [13]. The effect of the drug on I_{NaL} kinetics has not been previously studied and thus was examined in the present study. The decay of I_{NaL} was approximated by a double-exponential fit (Eq. 4 in the ESM; see examples in Fig. 5a) as previously suggested [12]. The fast component (τ_{BM} , tens of ms) represents burst mode (BM) and the slow component (τ_{LSM} , hundreds of ms) represents late scattered mode (LSM) of late Na^+ channel openings [12]. The effect of RAN (10 μM) on I_{NaL} was complex and reversible: the density was reduced (Fig. 6b) and the drug accelerated decay kinetics of both I_{NaL} components (Fig. 6c, d).

Effects of ranolazine on action potentials in myocytes from failing heart

The AP shape and its duration, especially the variability of AP duration, play an important role in abnormalities of the E-C coupling in HF. We previously showed that AP duration of ventricular myocytes is prolonged (at low rates) and AP duration variability is increased in this canine HF model and

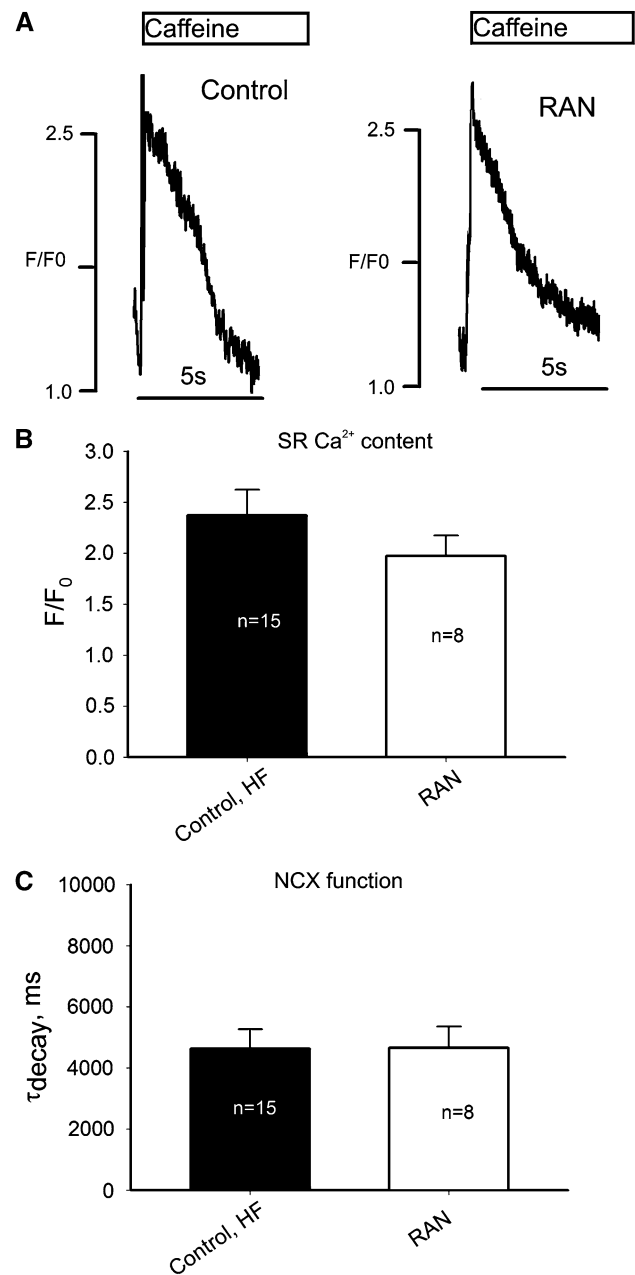


Fig. 5 Ranolazine affects SR Ca^{2+} content or NCX function insignificantly in ventricular myocytes from failing dog hearts. **a** Original traces of Ca^{2+} transients during the exposure to caffeine (10 mM) in control (*left panel*) and in the presence of ranolazine (RAN, 10 μM , *right panel*). **b** Average data for SR Ca^{2+} load, **c** average data for Ca^{2+} decay as a measure of NCX function (single exponential fit). Statistical analysis does not reveal a statistical difference between control and RAN for these parameters (ANOVA). *Data bars in b and c* represent mean \pm SEM pooled from 8 to 15 cells

in HF patients compared to NH, and the role of I_{NaL} in the AP duration abnormalities has been suggested [6, 7, 10]. Using the specific I_{NaL} inhibitor RAN allows further investigation of the role of I_{NaL} in AP regulation in HF. Accordingly, we determined the effects of RAN (10 μM) on AP duration and its variability at low and high pacing rates

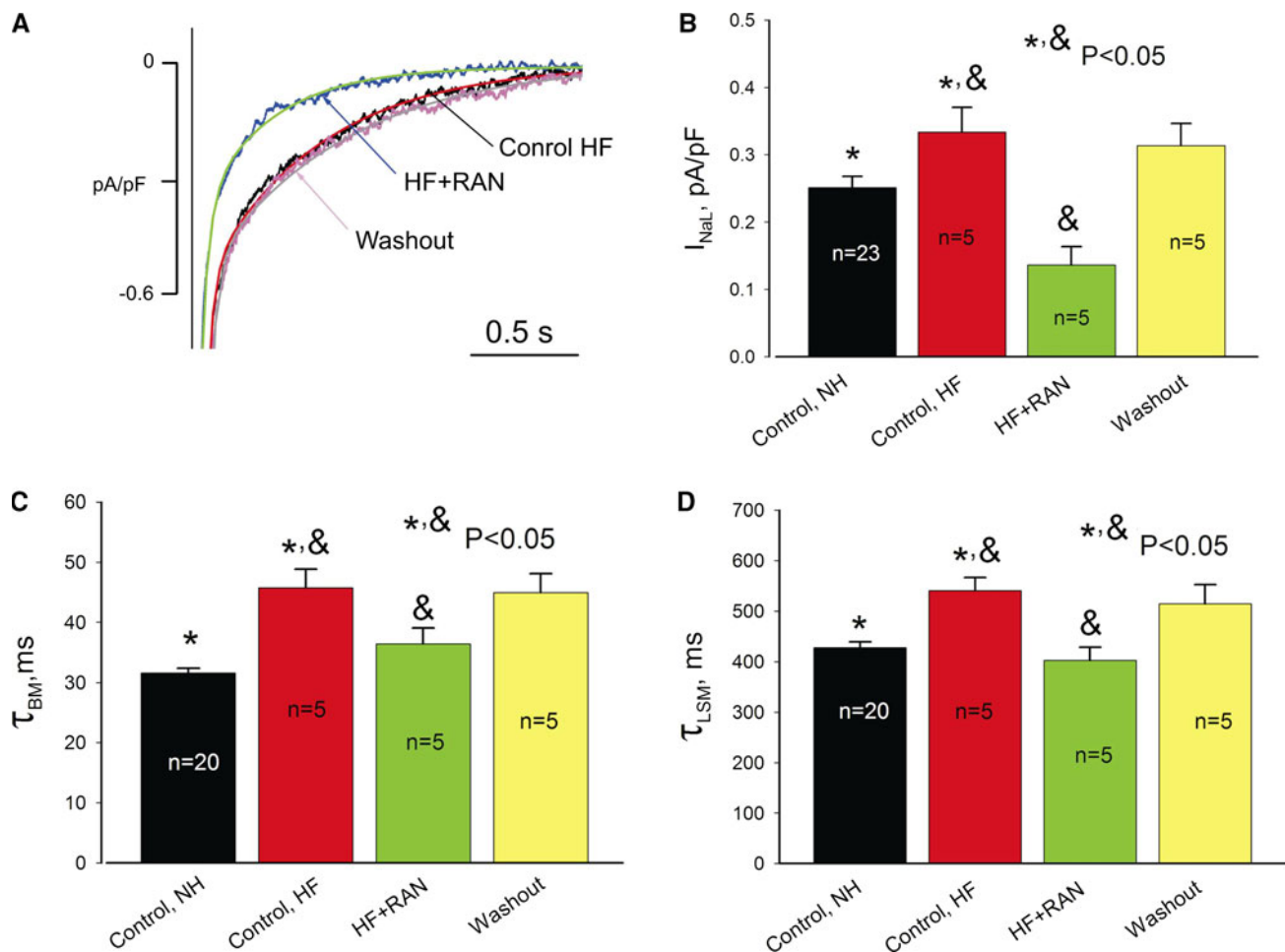


Fig. 6 Effects of RAN (10 μ M) on I_{NaL} in ventricular myocytes from canine failing hearts. **a** Representative traces along with double-exponential fit of the time course of I_{NaL} decay (solid lines). **b** Summary of the data on I_{NaL} density measured as a mean current

within 200–220 ms after the depolarization onset, and decay kinetics (**c**, **d**) measured at -30 mV in control, in the presence of RAN, and during the washout. Data are mean \pm SEM pooled from 5 to 23 cells. See details in text

in myocytes from failing hearts. The results of these experiments are summarized in Fig. 7. At both stimulation rates RAN effectively and reversibly shortened the prolonged APs and abolished the beat-to-beat variability apparent as a large dispersion in the AP duration distribution histograms (Fig. 7c–h). For comparison the AP duration and its dispersion in normal dog ventricular myocytes recorded at 0.25 and 1.5 Hz were 337 ± 52 ms (mean \pm SD, $n = 8$ cells) and 303 ± 40 ms ($n = 9$), respectively (data pooled from the previous publications [7, 9, 13]).

Numerical evaluation of I_{NaL} and late Na^+ influx during action potential plateau and its importance for the diastolic Ca^{2+} accumulation in HF

Based on our experimental data, we performed several numerical estimates to answer three key important questions:

1. What is the time course for I_{NaL} and late Na^+ influx (i.e., I_{NaL} integral) during AP plateau?

2. How much of this Na^+ influx could be blocked by 10 μ M of RAN?
3. Is late Na^+ influx sufficient to account for a major portion of diastolic cell Ca^{2+} accumulation observed experimentally during the pulse train at 1.5 Hz?

In the first approximation we used experimentally recorded AP traces to simulate Na^+ influx dynamics during AP plateau (above -30 mV) at low and high rates of

Fig. 7 RAN reversibly shortens the AP duration (APD) and reduces the dispersion of APD in ventricular myocytes from canine failing hearts. **a**, **b** Representative AP traces at low and high pacing rates recorded at the end of a pulse train, respectively. Dotted line indicates -30 mV level; APD values at this potential are indicated at the traces. **c–h** Histograms of the distribution of the APD measured at 90% of repolarization (APD₉₀). Bin sizes were 50 and 23 ms for **c**, **e**, **g** and for **d**, **f**, **h**, respectively. SD Standard deviation. APs were recorded in control (**c**, **d**), in the presence of 10 μ M RAN (**e**, **f**), and after RAN washout (**g**, **h**). Data were pooled from 6 to 12 cells of four failing hearts

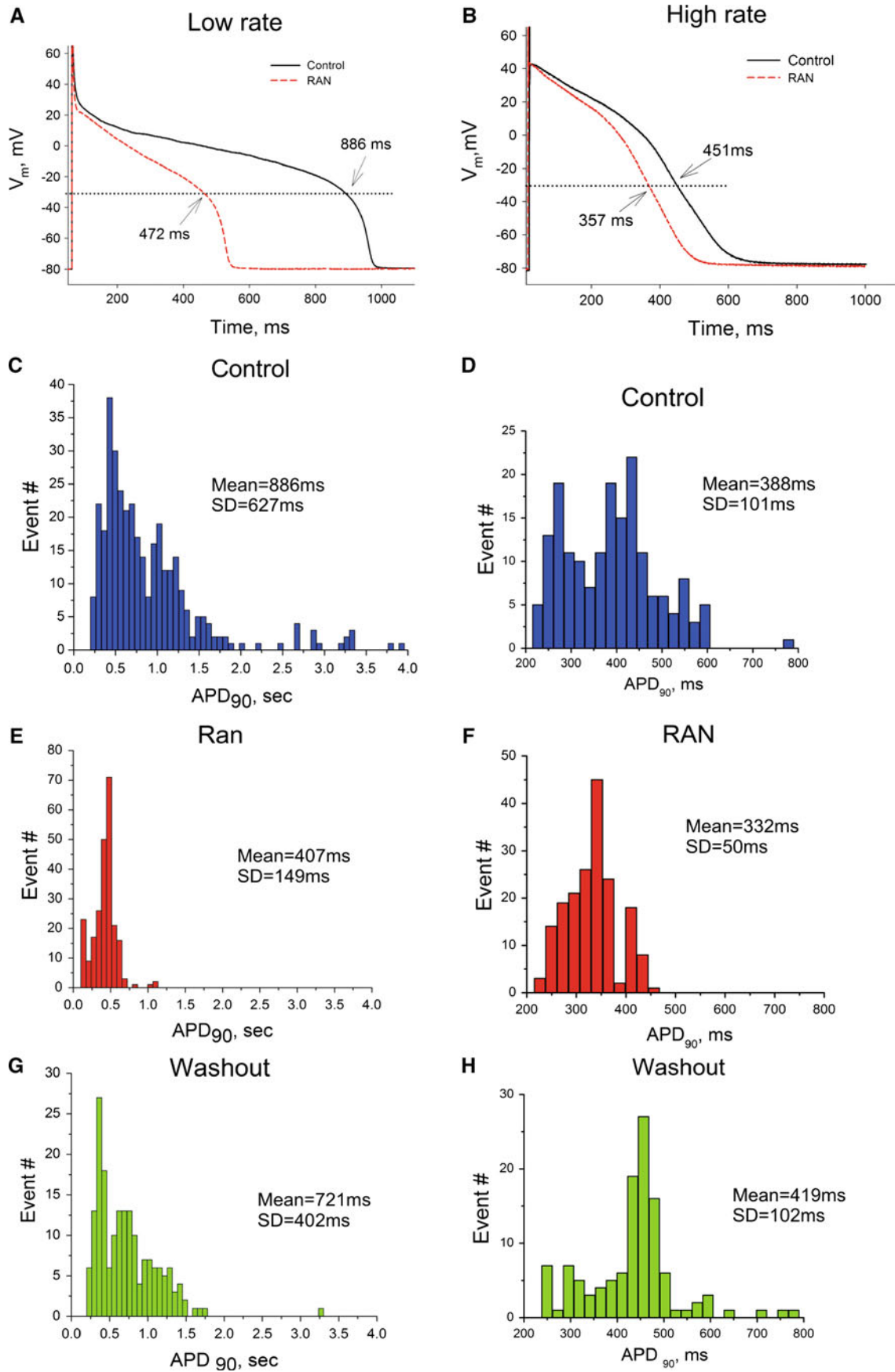
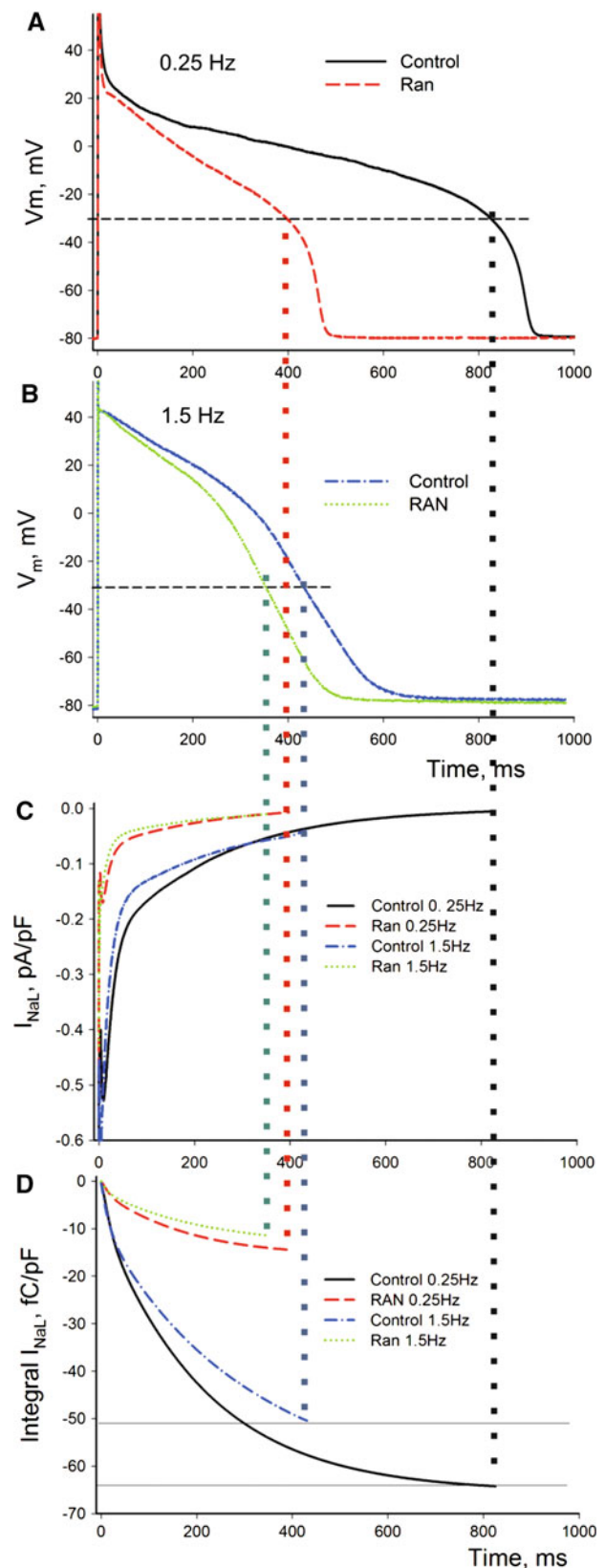


Fig. 8 AP-clamp numerical model. A substantial inhibition of I_{NaL} and late Na^+ influx (77%) during AP plateau by a therapeutic concentration (10 μM) of RAN. **a, b** Experimental AP recordings at low and high pacing rates in the absence or presence of RAN. **c, d** Predicted I_{NaL} and its integral (\sim late Na^+ influx) during the corresponding AP shapes (Eq. 9 in the ESM)

stimulation before and after RAN (Fig. 8a, b) (see formulations in the ESM). Results of these AP-clamp simulations are as follows: Because the model includes RAN-induced steady-state inactivation (SSI) shifts found at the physiological resting potential [13] (see Table 1 in the ESM), it predicts greater inhibition of I_{NaL} and late Na^+ influx by RAN in physiological conditions in comparison to the voltage-clamp data obtained from a very low holding potential (compare Figs. 6a, 8c). More specifically, RAN blocks about 77% of the late Na^+ influx during the single AP (from 64.3 to 14.5 fC/pF at low rate and from 50.4 to 11.5 fC/pF at the high rate).

A remarkable portion of late Na^+ influx is likely exchanged by NCX for Ca^{2+} steady state during stimulation at 1.5 Hz (Fig. 3) for the following reasons: (1) NCX function is enhanced in HF [16–18], (2) NCX operates in the reverse mode during AP plateau in canine failing myocytes (see Fig. 1f in [37]) and extrudes 3 Na^+ for influx of 1 Ca^{2+} , and (3) I_{NaL} blockade by RAN substantially reduces DCa (Fig. 3) but affects neither SR Ca^{2+} loading, nor NCX function (Fig. 5). Based on this reasoning, our numerical estimate demonstrates that the late Na^+ influx ($\sim I_{\text{NaL}}$ integral) during the AP plateau might be indeed substantial and sufficient to increase cytosolic $[\text{Ca}^{2+}]$ by ~ 72 nM assuming its efflux by the reverse $\text{Na}^+/\text{Ca}^{2+}$ exchange at the steady state during a 1.5 Hz stimulation train (see the ESM for detailed formulations and calculations). While our AP clamp simulations, described above, include real AP shapes of myocytes in our specific HF model, they only consider I_{NaL} , NCX, and cell Ca^{2+} buffering. Thus, the above 72 nM is likely a higher estimate because this simple estimate does not include possible contributions of other Ca^{2+} and Na^+ transport systems. Therefore, we further addressed the role on I_{NaL} in CaD accumulation in silico using our modified version of an established model for pacing-induced dog HF ventricular myocytes that includes all essential components of E-C coupling and Na^+ homeostasis [37]. This pacing-induced HF model produces similar remodeling of AP and ionic currents, including the augmented I_{NaL} , found in patients with HF and in our dog HF model [6–9, 37, 39]. The details of the model modification to include I_{NaL} are given in the ESM. The results of our model simulations are shown in Fig. 9. We applied a train of 11 stimulation pulses in the model and recorded intracellular Ca^{2+} dynamics and APs in



control and when I_{NaL} was set to zero. Our model simulations reproduced DCa accumulation (Fig. 9, upper panel) observed experimentally in failing myocytes (Fig. 3a, b, upper panels). Selective blockade of I_{NaL} in the model (either completely or partially, simulating RAN effect) shortened AP (Fig. 9, lower panel), and substantially reduced this simulated DCa accumulation similarly to that found in experiment (Figs. 7b–f, 3a, b, middle panels).

We next calculated the absolute cytosolic free Ca^{2+} dynamics during stimulation with the rate of 1.5 Hz from the respective Ca^{2+} signal traces represented originally by F/F_0 values (ESM). The CaT amplitude was 210–325 nM in myocytes from the HF model, i.e., values similar to those reported previously for myocytes from pacing-induced models of HF in dogs [37] (~200 nM, see also Fig. 7e) or cats [40] (~340 nM). Finally, from our experimental traces (examples in Fig. 3a, b), we found that during 1.5 Hz pulse trains RAN indeed suppresses the major portion of DCa accumulation, which in absolute terms of $[\text{Ca}^{2+}]$ ranges from 62 to 98 nM. Thus, both of our numerical simulations closely predict this experimental estimate for substantial DCa accumulation suppression by I_{NaL} inhibition.

Discussion

Using a combination of experimental and numerical modeling studies, we demonstrate at the single cell level that in

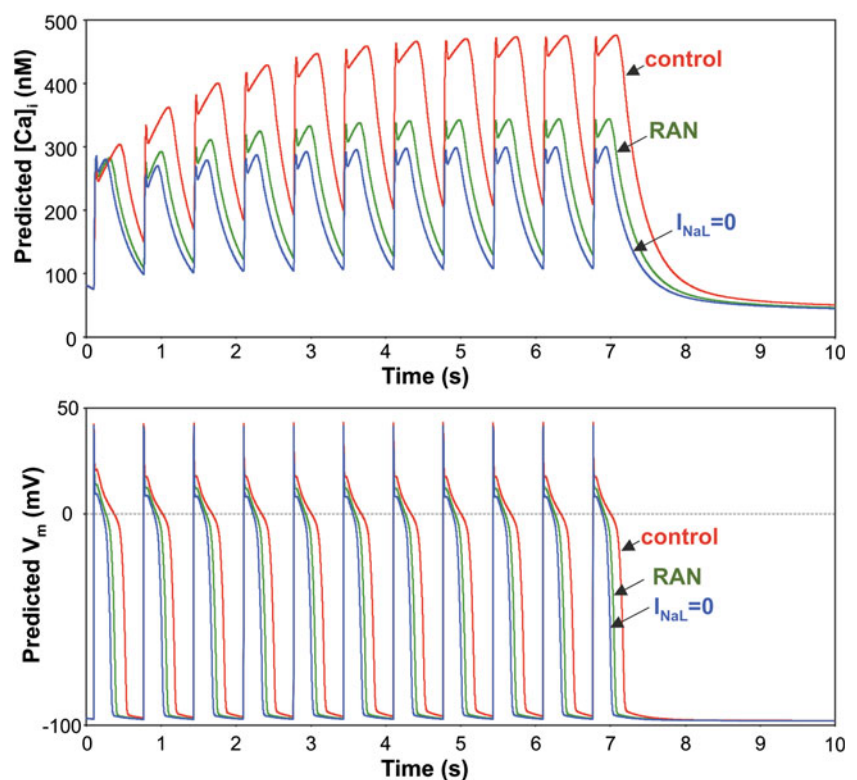
chronic HF augmented activity of the late Na^+ channels exerts both direct electrophysiological effects and indirect effects on intracellular Ca^{2+} concentration in ventricular myocytes. As discussed in detail below, our findings thus suggest a novel cellular and molecular mechanism contributing to rate-dependent [31, 32] impaired diastolic function (i.e., poor relaxation) and DAD-mediated triggered activity, two major abnormalities associated with chronic HF [2, 18, 41, 42]. As we noted in the Introduction, the previous suggestions about the I_{NaL} -mediated mechanism in HF were based on results obtained in normal myocardium using *Anemonia sulcata* toxin, ATX-II, to produce persistent I_{Na} [27, 28]. The role of I_{NaL} in these latter studies could be exaggerated because ATX-II caused a fivefold increase in the persistent I_{Na} (Fig. 4a in [28]), whereas studies in failing human and dog hearts showed I_{NaL} amplitude increases of 30–50% [8, 9].

Specific mechanisms to improve Ca^{2+} handling and heart contractility by inhibition of late Na^+ current

Diastolic Ca^{2+} accumulation

Previous studies in animal models of HF showed that partial blockade of either total Na^+ current by saxitoxin or I_{NaL} by RAN improved contractility of myocytes from failing hearts [6, 13]. The results of the present study support the following specific mechanisms of late Na^+

Fig. 9 In silico demonstration of the role of the augmented I_{NaL} in AP shape and diastolic Ca^{2+} accumulation in canine failing ventricular myocytes. Numerically simulated dynamics of intracellular Ca^{2+} concentration ($[\text{Ca}^{2+}]_i$) (upper panel) in a train of 11 pulses applied with a rate of 1.5 Hz. Complete I_{NaL} elimination or reduction by RAN (10 μM) substantially reduces the diastolic Ca^{2+} accumulation and shortens AP duration (lower panel). Simulations were performed using a modified Winslow et al. E-C coupling model of failing canine ventricular myocytes [37] (see details in the ESM)



current contribution to abnormal Ca^{2+} handling and impaired contraction in chronic HF. Increased I_{NaL} in HF alters AP and simultaneously provides a substantial systolic late Na^+ influx (during AP plateau). These two effects combined likely cause or modulate Ca^{2+} influx via the reverse mode $\text{Na}^+/\text{Ca}^{2+}$ exchange. This additional I_{NaL} -dependent systolic Ca^{2+} influx contributes to major abnormalities of cell Ca^{2+} handling, including DCa accumulation (compare upper panels in Figs. 1b and 3b), Ca^{2+} alternans (Fig. 3a, upper panel), and SCaR (Fig. 4). While the DCa accumulation and Ca^{2+} alternans can directly impair contractions of individual myocytes, increased rate of SCaRs can further worsen the diastolic cardiac muscle function. Indeed, heterogeneity of diastolic $[\text{Ca}^{2+}]_i$ among cells within myocardial tissue caused by asynchronous SCaRs leads to heterogeneous myofilament activation, the summation of which produces a Ca^{2+} -dependent component to diastolic tone [43].

The idea that I_{NaL} and its related Na^+ influx cause a dynamic cell Ca^{2+} accumulation in HF is supported by the following results. We showed that partial blockade of I_{NaL} by RAN or TTX greatly improves Ca^{2+} handling in failing myocytes specifically; associated with inhibition of I_{NaL} , the DCa accumulation decreased (Fig. 3), alternans disappeared (Fig. 3a), and the probability of SCaRs decreased substantially (\sim threefold) (Fig. 4). This idea is also supported by recent studies in ventricular muscle strips isolated from end-stage failing human hearts [28] and in myocytes from dog failing hearts [13], which demonstrated that inhibition of I_{NaL} by RAN significantly reduces frequency-dependent increase in diastolic tension (i.e., diastolic dysfunction) by approximately 30% (in line with our results). Finally, inhibition of I_{NaL} and I_{NaL} -related Na^+ influx in silico (both an AP clamp and a complete model of E-C coupling) substantially and selectively suppresses DCa accumulation of the myocytes of failing hearts (Figs. 7, 9).

Dynamic Ca^{2+} cycling abnormalities in failing heart; alternans and spontaneous Ca^{2+} releases

At a low stimulation rate of 0.25 Hz we also observed an abnormal tonic or dome component of CaT (compare upper panels in Figs. 1a, 2a, b) (first reported in heart ventricular muscle strips from patients with HF [44]). In addition we found some Ca^{2+} oscillations at low pacing rates (Fig. 2a upper panel) and beat-to-beat variations of Ca^{2+} transients at higher rates of stimulation (Fig. 3a, upper panel) that may be a sign of alternans of intracellular Ca^{2+} cycling [45]. TTX (middle panels in Fig. 2b) or RAN (middle panels in Fig. 2a) reversed these abnormalities.

The threshold for SCaR is lower in HF because of reduced SERCA function and increased SR Ca^{2+} leak [20, 21] in line with observation of SCaRs in our recordings in

failing (Fig. 4) but not in normal myocytes (Fig. 1b). Diastolic SCaRs can initiate DADs via activation of the forward mode NCX inward current, and/or nonselective channels [18, 25]. Previous studies demonstrated that when SCaRs within a cardiomyocyte are sufficiently synchronized (e.g., multifocal Ca^{2+} waves), the resultant depolarization summates and can be sufficient to trigger a spontaneous AP [43]. The amplitude of SCaRs ($F/F_0 \sim 1.55$) is close to that of CaT during 1.5 Hz pacing (Fig. 4a), which could be pro-arrhythmic, especially in the context of up-regulated NCX in HF [16–18]. Indeed, it has been documented that the threshold amplitude of SCaRs that is sufficient to evoke DADs is almost twofold lower for HF myocytes (~ 280 nM) compared to that in normal heart (~ 512 nM) [42]. This threshold is close to the amplitude of SCaRs reported here (~ 250 nM) (Fig. 4a). Increased Ca^{2+} entry is an established mechanism for SCaR from the SR [46]. Thus, the DCa accumulation represents a reasonable mechanism for SCaR after the pulse train in our chronic HF model. The fact that TTX and/or RAN inhibited SCaRs without significantly affecting SR load and NCX function (Fig. 5) supports this mechanism (Fig. 4b, c). On the other hand, small (albeit insignificant) decrease in SR Ca^{2+} load in the presence of RAN (Fig. 5b) does not completely rule out some involvement of SR load in SCaR occurrence, given the non-linear behavior of the SR (i.e., a relatively small change in load triggers the release) [47]. Also elucidation of possible contributions of changes in AP shape and duration in the improvement of Ca^{2+} handling, caused by the I_{NaL} reduction shown both experimentally and in silico (Figs. 7, 9), merits consideration in future studies.

Predictions in silico

Our model simulations provide quantitative evidence that I_{NaL} accounts for a major portion of diastolic cell Ca^{2+} accumulation in myocytes (stimulated at rate of 1.5 Hz) measured experimentally. A simplified numerical modeling of I_{NaL} during AP clamp shows that RAN (10 μM) almost completely (by 77%) inhibits late Na^+ influx (Fig. 8d). At the same time we also show that Na^+ influx via I_{NaL} can be indeed substantial. Taking into account that NCX operates in the reverse mode during AP in HF [24, 48] and NCX function is enhanced in HF [16–18], we reasoned that a large portion of Na^+ influx is likely to be the cause of an increase in the dynamic exchanged by the reverse mode NCX for Ca^{2+} . It is known, for example, that the reverse mode NCX-mediated Ca^{2+} influx is indeed substantial and may even result in the direct activation of contraction in HF [48]. We estimated that late Na^+ influx is sufficient to cause a 72 nM increase in cytosolic $[\text{Ca}^{2+}]$ via this mechanism. We also tested the effect of I_{NaL} inhibition in

in silico simulations of the E-C coupling process including all substantial mechanisms involved in the regulation of the Ca^{2+} and Na^+ homeostasis in HF (Fig. 9). Our model simulations closely reproduce our experimental results and confirm the importance of I_{NaL} for both the AP duration and the DCa accumulation in failing myocardium.

Physiological significance, clinical relevance

In a recent clinical trial RAN significantly reduced arrhythmias in patients with non ST-segment elevation acute coronary syndrome [49] pointing to a potential clinical relevance of I_{NaL} . The beneficial effect of RAN in these patients can be thus explained, in part, by two mechanisms: (1) improvement of repolarization shown in previous studies [13, 33] and in this study (see Fig. 6) and (2) Ca^{2+} handling associated with a decreased probability of spontaneous releases (shown in this study, Fig. 4) and, hence, DADs and their triggered APs (see previous section). Partial inhibition of I_{NaL} by RAN, TTX, or saxitoxin greatly improves repolarization and decreases intrinsic beat-to-beat AP duration variability of failing cardiomyocytes [7, 9, 13] (Fig. 6). The cellular mechanisms of RAN effects proposed in this study may explain, at least in part, beneficial RAN effects previously reported in whole-animal studies by our group and others. In dogs and rabbits RAN reduced infarct size and Ca^{2+} overload in response to a regional ischemia-reperfusion [50, 51]. In dogs with coronary microembolization-induced HF, acute intravenous administration of RAN improved LV systolic function and LV mechanical efficiency without increasing myocardial oxygen consumption and without any increase in heart rate or reduction of systemic blood pressure [52].

I_{NaL} as a novel therapeutic target

The emerging paradigm with regard to Na^+ channels in HF is that I_{NaT} is decreased [8, 14, 15] but simultaneously I_{NaL} is increased [5]. Blockers of I_{NaT} are pro-arrhythmic in HF because they will further slow conduction, thus worsening impulse conduction [53] and thereby facilitating development of re-entry. Hence, transient and late Na^+ currents must be treated differently. The new type of “smart” drugs should preferentially block I_{NaL} over I_{NaT} [5, 54, 55]. The potential benefits (preventing Ca^{2+} overload and arrhythmias) of the preferential I_{NaL} blockade can be also expected in hypoxia and ischemia, in which I_{NaL} increase and Na^+ -induced Ca^{2+} overload are major features. In ischemia, accumulation of toxic metabolite lysophosphatidylcholine and reactive oxygen species dramatically increases I_{NaL} [56–58]. Indeed Na^+ channels are critically involved in this process because their blockers or activators reduce or

increase Ca^{2+} overload in these pathological conditions, respectively [59, 60].

In conclusion, we provide evidence that I_{NaL} and its systolic Na^+ influx contribute to the dynamic DCa accumulation and spontaneous release in ventricular myocytes from dog model of chronic HF. Therefore, the results of the present study support the idea that selective blockade of this Na^+ current represents a plausible strategy to treat Ca^{2+} -related diastolic dysfunction and arrhythmia in HF.

Acknowledgments This study was supported by grants from the NIH (HL074328, A. Undrovinas), American Heart Association (0350472Z, A. Undrovinas), Gilead Palo Alto Inc. (A. Undrovinas), and by the Intramural Research Program of the NIH, National Institute on Aging (V. A. Maltsev).

Conflict of interest statement Dr. A. Undrovinas reports research support from Gilead Palo Alto, Inc., and Dr. L. Belardinelli is an employee of Gilead Palo Alto Inc. All other authors report no conflicts.

References

- Bers DM (2006) Altered cardiac myocyte Ca regulation in heart failure. *Physiology* (Bethesda) 21:380–387
- Hasenfuss G, Schillinger W, Lehnart SE, Preuss M, Pieske B, Maier LS et al (1999) Relationship between Na^+ - Ca^{2+} -exchanger protein levels and diastolic function of failing human myocardium. *Circulation* 99:641–648
- Pieske B, Maier LS, Piacentino V 3rd, Weisser J, Hasenfuss G, Houser S (2002) Rate dependence of $[\text{Na}^+]_i$ and contractility in nonfailing and failing human myocardium. *Circulation* 106:447–453
- Hobai IA, Maack C, O'Rourke B (2004) Partial inhibition of sodium/calcium exchange restores cellular calcium handling in canine heart failure. *Circ Res* 95:292–299
- Maltsev VA, Undrovinas A (2008) Late sodium current in failing heart: friend or foe? *Prog Biophys Mol Biol* 96:421–451
- Maltsev VA, Sabbah HN, Higgins RSD, Silverman N, Lesch M, Undrovinas AI (1998) Novel, ultraslow inactivating sodium current in human ventricular cardiomyocytes. *Circulation* 98:2545–2552
- Undrovinas AI, Maltsev VA, Sabbah HN (1999) Repolarization abnormalities in cardiomyocytes of dogs with chronic heart failure: role of sustained inward current. *Cell Mol Life Sci* 55:494–505
- Valdivia CR, Chu WW, Pu J, Foell JD, Haworth RA, Wolff MR et al (2005) Increased late sodium current in myocytes from a canine heart failure model and from failing human heart. *J Mol Cell Cardiol* 38:475–483
- Maltsev VA, Silverman N, Sabbah HN, Undrovinas AI (2007) Chronic heart failure slows late sodium current in human and canine ventricular myocytes: implications for repolarization variability. *Eur J Heart Fail* 9:219–227
- Maltsev VA, Sabbah HN, Tanimura M, Lesch M, Goldstein S, Undrovinas AI (1998) Relationship between action potential, contraction-relaxation pattern, and intracellular Ca^{2+} transient in cardiomyocytes of dogs with chronic heart failure. *Cell Mol Life Sci* 54:597–605
- Undrovinas AI, Maltsev VA, Kyle JW, Silverman NA, Sabbah HN (2002) Gating of the late Na^+ channel in normal and failing human myocardium. *J Mol Cell Cardiol* 34:1477–1489

12. Maltsev VA, Undrovinas AI (2006) A multi-modal composition of the late Na^+ current in human ventricular cardiomyocytes. *Cardiovasc Res* 69:116–127
13. Undrovinas AI, Belardinelli L, Undrovinas NA, Sabbah HN (2006) Ranolazine improves abnormal repolarization and contraction in left ventricular myocytes of dogs with heart failure by inhibiting late sodium current. *J Cardiovasc Electrophysiol* 17:S169–S177
14. Maltsev VA, Sabbah HN, Undrovinas AI (2002) Down-regulation of sodium current in chronic heart failure: effects of long-term therapy with carvedilol. *Cell Mol Life Sci* 59:1561–1568
15. Zicha S, Maltsev VA, Nattel S, Sabbah HN, Undrovinas AI (2004) Post-transcriptional alterations in the expression of cardiac Na^+ channel subunits in chronic heart failure. *J Mol Cell Cardiol* 37:91–100
16. Studer R, Reinecke H, Bilger J, Eschenhagen T, Bohm M, Hasenfuss G et al (1994) Gene expression of the cardiac $\text{Na}^+-\text{Ca}^{2+}$ exchanger in end-stage human heart failure. *Circ Res* 75:443–453
17. Flesch M, Schwinger RH, Schiffer F, Frank K, Sudkamp M, Kuhn-Regnier F et al (1996) Evidence for functional relevance of an enhanced expression of the $\text{Na}^+-\text{Ca}^{2+}$ exchanger in failing human myocardium. *Circulation* 94:992–1002
18. Pogwizd SM, Schlotthauer K, Li L, Yuan W, Bers DM (2001) Arrhythmogenesis and contractile dysfunction in heart failure: roles of sodium-calcium exchange, inward rectifier potassium current, and residual beta-adrenergic responsiveness. *Circ Res* 88:1159–1167
19. Brillantes AM, Allen P, Takahashi T, Izumo S, Marks AR (1992) Differences in cardiac calcium release channel (ryanodine receptor) expression in myocardium from patients with end-stage heart failure caused by ischemic versus dilated cardiomyopathy. *Circ Res* 71:18–26
20. Bers DM, Eisner DA, Valdivia HH (2003) Sarcoplasmic reticulum Ca^{2+} and heart failure: roles of diastolic leak and Ca^{2+} transport. *Circ Res* 93:487–490
21. Belevych A, Kubalova Z, Terentyev D, Hamlin RL, Carnes CA, Gyorke S (2007) Enhanced ryanodine receptor-mediated calcium leak determines reduced sarcoplasmic reticulum calcium content in chronic canine heart failure. *Biophys J* 93:4083–4092
22. Hobai IA, O'Rourke B (2001) Decreased sarcoplasmic reticulum calcium content is responsible for defective excitation-contraction coupling in canine heart failure. *Circulation* 103:1577–1584
23. Piacentino V 3rd, Weber CR, Chen X, Weisser-Thomas J, Margulies KB, Bers DM et al (2003) Cellular basis of abnormal calcium transients of failing human ventricular myocytes. *Circ Res* 92:651–658
24. Baartscheer A, Schumacher CA, Belterman CN, Coronel R, Fioret JW (2003) $[\text{Na}^+]_i$ and the driving force of the $\text{Na}^+/\text{Ca}^{2+}$ -exchanger in heart failure. *Cardiovasc Res* 57:986–995
25. Clusin WT (2003) Calcium and cardiac arrhythmias: DADs, EADs, and alternans. *Crit Rev Clin Lab Sci* 40:337–375
26. Gwathmey JK, Slawsky MT, Briggs GM, Morgan JP (1988) Role of intracellular sodium in the regulation of intracellular calcium and contractility. Effects of DPI 201-106 on excitation-contraction coupling in human ventricular myocardium. *J Clin Invest* 82:1592–1605
27. Fraser H, Belardinelli L, Wang L, Light PE, McVeigh JJ, Clanachan AS (2006) Ranolazine decreases diastolic calcium accumulation caused by ATX-II or ischemia in rat hearts. *J Mol Cell Cardiol* 41:1031–1038
28. Sossalla S, Wagner S, Rasenack EC, Ruff H, Weber SL, Schondube FA et al (2008) Ranolazine improves diastolic dysfunction in isolated myocardium from failing human hearts—role of late sodium current and intracellular ion accumulation. *J Mol Cell Cardiol* 14:14
29. Lindegger N, Hagen BM, Marks AR, Lederer WJ, Kass RS (2009) Diastolic transient inward current in long QT syndrome type 3 is caused by Ca^{2+} overload and inhibited by ranolazine. *J Mol Cell Cardiol* 47:326–334
30. Sabbah HN, Goldberg AD, Schoels W, Kono T, Webb C, Brachmann J et al (1992) Spontaneous and inducible ventricular arrhythmias in a canine model of chronic heart failure: relation to haemodynamics and sympathoadrenergic activation. *Eur Heart J* 13:1562–1572
31. Rao K, Fisher ML, Robinson S, Shorofsky S, Gottlieb SS (2007) Effect of chronic changes in heart rate on congestive heart failure. *J Card Fail* 13:269–274
32. Logeart D, Gueffet JP, Rouzet F, Pousset F, Chavelas C, Solal AC et al (2009) Heart rate per se impacts cardiac function in patients with systolic heart failure and pacing: a pilot study. *Eur J Heart Fail* 11:53–57
33. Antzelevitch C, Belardinelli L, Zygmunt AC, Burashnikov A, Di Diego JM, Fish JM et al (2004) Electrophysiological effects of ranolazine, a novel antianginal agent with antiarrhythmic properties. *Circulation* 110:904–910
34. Maltsev VA, Sabbah HN, Undrovinas AI (2001) Late sodium current is a novel target for amiodarone: studies in failing human myocardium. *J Mol Cell Cardiol* 33:923–932
35. Nagatomo T, January CT, Makielski JC (2000) Preferential block of late sodium current in the LQT3 DeltaKPK mutant by the class I(C) antiarrhythmic flecainide. *Mol Pharmacol* 57:101–107
36. Dumaine R, Wang Q, Keating MT, Hartmann HA, Schwartz PJ, Brown AM et al (1996) Multiple mechanisms of Na^+ channel-linked long-QT syndrome. *Circ Res* 78:916–924
37. Winslow RL, Rice J, Jafri S, Marban E, O'Rourke B (1999) Mechanisms of altered excitation-contraction coupling in canine tachycardia-induced heart failure, II: model studies. *Circ Res* 84:571–586
38. Bers DM (2002) Cardiac excitation-contraction coupling. *Nature* 415:198–205
39. Kaab S, Nuss HB, Chiamvimonvat N, O'Rourke B, Pak PH, Kass DA et al (1996) Ionic mechanism of action potential prolongation in ventricular myocytes from dogs with pacing-induced heart failure. *Circ Res* 78:262–273
40. Harris DM, Mills GD, Chen X, Kubo H, Berretta RM, Votaw VS et al (2005) Alterations in early action potential repolarization causes localized failure of sarcoplasmic reticulum Ca^{2+} release. *Circ Res* 96:543–550
41. Wigle ED (1995) The failing heart. In: Diastolic dysfunction: pathology and treatment options. Lippincott-Raven, Philadelphia, pp 79–94
42. Pogwizd SM, Bers DM (2002) Na/Ca exchange in heart failure: contractile dysfunction and arrhythmogenesis. *Ann N Y Acad Sci* 976:454–465
43. Lakatta EG (1992) Functional implications of spontaneous sarcoplasmic reticulum Ca^{2+} release in the heart. *Cardiovasc Res* 26:193–214
44. Gwathmey JK, Copelas L, MacKinnon R, Schoen FJ, Feldman MD, Grossman W et al (1987) Abnormal intracellular calcium handling in myocardium from patients with end-stage heart failure. *Circ Res* 61:70–76
45. Wilson LD, Wan X, Rosenbaum DS (2006) Cellular alternans: a mechanism linking calcium cycling proteins to cardiac arrhythmogenesis. *Ann N Y Acad Sci* 1080:216–234
46. Johnson N, Danilo P Jr, Wit AL, Rosen MR (1986) Characteristics of initiation and termination of catecholamine-induced triggered activity in atrial fibers of the coronary sinus. *Circulation* 74:1168–1179
47. Diaz ME, Trafford AW, O'Neill SC, Eisner DA (1997) Measurement of sarcoplasmic reticulum Ca^{2+} content and

- sarcolemmal Ca^{2+} fluxes in isolated rat ventricular myocytes during spontaneous Ca^{2+} release. *J Physiol* 501:3–16
48. Weisser-Thomas J, Piacentino V 3rd, Gaughan JP, Margulies K, Houser SR (2003) Calcium entry via Na/Ca exchange during the action potential directly contributes to contraction of failing human ventricular myocytes. *Cardiovasc Res* 57:974–985
 49. Scirica BM, Morrow DA, Hod H, Murphy SA, Belardinelli L, Hedgepeth CM et al (2007) Effect of ranolazine, an antianginal agent with novel electrophysiological properties, on the incidence of arrhythmias in patients with non ST-segment elevation acute coronary syndrome: results from the Metabolic Efficiency With Ranolazine for Less Ischemia in Non ST-Elevation Acute Coronary Syndrome Thrombolysis in Myocardial Infarction 36 (MERLIN-TIMI 36) randomized controlled trial. *Circulation* 116:1647–1652
 50. Black SC, Gralinski MR, McCormack JG, Driscoll EM, Lucchesi BR (1994) Effect of ranolazine on infarct size in a canine model of regional myocardial ischemia/reperfusion. *J Cardiovasc Pharmacol* 24:921–928
 51. Gralinski MR, Black SC, Kilgore KS, Chou AY, McCormack JG, Lucchesi BR (1994) Cardioprotective effects of ranolazine (RS-43285) in the isolated perfused rabbit heart. *Cardiovasc Res* 28:1231–1237
 52. Chandler MP, Stanley WC, Morita H, Suzuki G, Roth BA, Blackburn B et al (2002) Short-term treatment with ranolazine improves mechanical efficiency in dogs with chronic heart failure. *Circ Res* 91:278–280
 53. Shah M, Akar FG, Tomaselli GF (2005) Molecular basis of arrhythmias. *Circulation* 112:2517–2529
 54. Undrovinas AI, Maltsev VA, Higgins RSD, Silverman N, Goldstein S, Sabbah HN (2000) Amiodarone blocks the late sodium current in isolated ventricular myocytes of explanted failed human hearts. *J Am Coll Cardiol* 35:97A
 55. Undrovinas A, Maltsev VA (2008) Late sodium current is a new therapeutic target to improve contractility and rhythm in failing heart. *Cardiovasc Hematol Agents Med Chem* 6:348–359
 56. Undrovinas AI, Fleidervish IA, Makielski JC (1992) Inward sodium current at resting potentials in single cardiac myocytes induced by the ischemic metabolite lysophosphatidylcholine. *Circ Res* 71:1231–1241
 57. Beresewicz A, Horackova M (1991) Alterations in electrical and contractile behavior of isolated cardiomyocytes by hydrogen peroxide: possible ionic mechanisms. *J Mol Cell Cardiol* 23:899–918
 58. Song Y, Shryock JC, Wagner S, Maier LS, Belardinelli L (2006) Blocking late sodium current reduces hydrogen peroxide-induced arrhythmogenic activity and contractile dysfunction. *J Pharmacol Exp Ther* 318:214–222
 59. Haigney MC, Lakatta EG, Stern MD, Silverman HS (1994) Sodium channel blockade reduces hypoxic sodium loading and sodium-dependent calcium loading. *Circulation* 90:391–399
 60. Ver Donck L, Borgers M (1991) Myocardial protection by R 56865: a new principle based on prevention of ion channel pathology. *Am J Physiol* 261:H1828–H1835